Int J Earth Sci (Geol Rundsch) (2006) 95: 355–369
DOI 10.1007/s00531-005-0054-6

ORIGINAL PAPER

M. Zhai · A. B. Kampunzu · M. P. Modisi · Z. Bagai

Sr and Nd isotope systematics of Francistown plutonic rocks, Botswana: implications for Neoarchaean crustal evolution of the Zimbabwe craton

Received: 14 July 2004 / Accepted: 4 September 2005 / Published online: 14 December 2005

Abstract The Francistown plutonic rocks at the south-western margin of the Zimbabwe craton consist of three igneous suites: Sanukitoid, Tonalite–Trondhjemite–Granite (TTG) suites and High-K granites. The TTG suite is subdivided into High Aluminum-TTG (HA-TTG) and Low Aluminum-TTG (LA-TTG) sub-suites. Their Rb–Sr isotope systems were partially homogenized by post-crystallization thermo–tectonic events, in which hydrothermal solutions and migmatization played an important role. Therefore, the Rb–Sr isochron age of 2427 ± 54 Ma can only be regarded as a lower limit to the Francistown plutonic rock age. The large errors in the Sm–Nd isochron dates of Francistown granitoids indicate that these dates are not really constrained. In this study we compared the rock types of Francistown and adjacent areas, adopting the precise U, Th–Pb single zircon SHRIMP ages from the Vumba area as references. For TTG and Sanukitoid suites, the age we adopted is ca. 2.7 Ga, which is close to their depleted-mantle Sm–Nd model ages (T_{DM}). For High-K granites, the age adopted is ca. 2.65 Ga, which is also close to their Sm–Nd isochron age. The highest ε^t_{Nd} values of Sanukitoids and TTG are +2.1 and +2.3, respectively. The positive ε^t_{Nd} values and trace element geochemistry support partial melting of a depleted mantle and young oceanic crust for the genesis of Sanukitoid and the TTG suites respectively. The lowest ε^t_{Nd} values of Sanukitoids and TTGs are −1.0 and −1.1, respectively, indicating contamination by continental crust, up to 10 and 14%, respectively. The ε^t_{Nd} values of TTG decrease with decreasing Al_2O_3 and Sr contents and increasing Eu negative anomalies (Eu*–Eu), suggesting that the TTG magmas underwent a coupled fractionation crystallization and crustal contamination, and that the LA-TTG was the product of the fractionation and contamination of the HA-TTG sub-suite. In contrast, negative ε^t_{Nd} values for the High-K granites (from −0.4 to −3.5) indicate the involvement of LA-TTG and some materials from an old continental crust in their genesis. The products of partial melting of both oceanic and continental crusts at the south-western margin of the Zimbabwe craton occurred within a short time interval (from 2.7 to 2.65 Ga ago) suggesting that the Francistown plutonic rocks were formed in a active continental margin environment, where a young ocean plate (Limpopo oceanic plate) subducted underneath an old continental plate (Zimbabwe craton).

Keywords Rb–Sr isotopes · Sm–Nd isotopes · Petrogenesis · Tectonic evolution · Archaean TTG–Sanukitoid–High-K granites · Francistown · Botswana

M. Zhai (✉) · A. B. Kampunzu · M. P. Modisi · Z. Bagai
Department of Geology, University of Botswana,
P. Bag 0022, Gaborone, Botswana
E-mail: zhaim@mopipi.ub.bw
Fax: +267-318-5097

Introduction

Archaean granite–greenstone terrains are important for the understanding of continental crust development and Earth's early evolution history (Hughes 1982). Furthermore, they frequently host major ore deposits such as Au, Cu, Ni (e.g. Roberts and Sheaham 1988; Evans 1993; Chatupa 1999). The Zimbabwe craton (Fig. 1a) preserves one of the earliest Archaean continental crusts known in the world (Dodson et al. 1988, 2001; Nägler et al. 1997; Frei et al. 1999; Horstwood et al. 1999; Dirks and Jelsma 2002). Previous studies (e.g. Tombale 1992; Bickle et al. 1993; Mkewli et al. 1995; Kusky 1998; Jelsma and Dirks 2000) led to two distinct geotectonic interpretations for the Neoarchaean evolution of the Zimbabwe craton. The plume-rift related model (e.g. Condie 1975; Bickle et al. 1993) suggests that the formation of the craton was due to continental rifting and mantle plume activities or rifting in a back-arc environment. Kusky (1998) and Bagai et al. (2002) challenged this model, and made the connection between the emplacement of granite–greenstone terrains and the

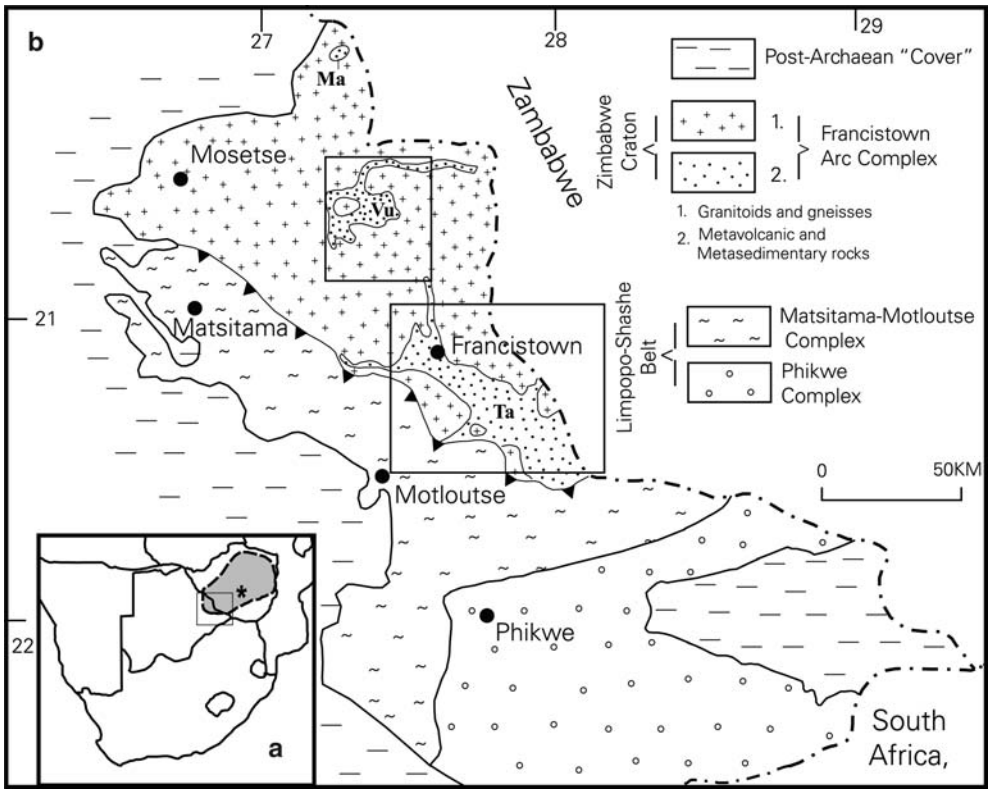

Fig. 1 **a** Location of the Zimbabwe craton in southern Africa. The *gray area* represents the Zimbabwe craton. The *asterisk* indicates the locality of the Tokwe nucleus, where the oldest crustal rocks are preserved. The *rectangle* shows the area of **b**. **b** Map showing the main geological units of southern Zimbabwe craton and adjacent area in northeast Botswana (Modified from McCourt et al. 2004). The *larger rectangle* locates the area of Fig. 2, and the *smaller rectangle* locates the study area of Bagai et al. (2002). There are three typical greenstone belts in the Francistown arc complex: *Ta*, Tati Volcanic Group; *Vu*, Vumba Volcanic Group; *Ma*, Maitengwe Volcanic Group. The boundary separating the Matsitama–Motloutse complex from the Francistown arc complex is the thrust sense Shashe shear zone with the teeth on this boundary indicating the upper plate

subduction of an oceanic plate. Kusky (1998) suggested that the greenstone belts aligned along the southern part of the Zimbabwe craton represent an oceanic suture which closed at ca. 2.70 Ga. Plate convergence models are consistent with the Zimbabwe craton shortening and Neoarchaean northward thrusting of the Limpopo Belt (e.g. Coward et al. 1976; Wilson 1990; McCourt and Vearncombe 1992; McCourt et al. 2004). The Francistown arc complex is located at the southwest margin of the Zimbabwe craton (McCourt et al. 2004), next to the Limpopo belt (Fig. 1b), making it a key area in the formation and evolution of the Zimbabwe craton.

Kampunzu et al. (2003) studied major and trace element geochemical characteristics of the Francistown granitoids and identified three magmatic suites: Trondhjemite–Tonalite–Granite, Sanukitoid and High-K granite suites. On the basis of major and trace element data, these authors related the magmatic suites to a plate convergence initiated by a northward subduction of the "Limpopo" oceanic plate underneath a continental block that includes the Francistown arc complex. The evolution from TTG to Sanukitoids to High-K granites indicates a progressive change from an earlier, flat subduction of a hot lithosphere to a steeper subduction and finally to slab detachment and extensional collapse. These interpretations need to be substantiated and tested with studies from other fields, especially that of isotope geochemistry. Although the published geochronological dates listed in Table 1 indicates a Neoarchaean age for the Francistown granitoids, available data is very limited. Specifically, since Sr, K, and Rb are mobile elements, Rb–Sr and K–Ar dates in old rocks are frequently influenced by post-crystallization processes, e.g. metamorphism or alteration (e.g. Faure 1986). Therefore, in order to conclusively establish the geological evolution of the Zimbabwe craton in NE Botswana, more isotopic data, especially of the immobile elements such as Sm–Nd, are necessary.

The objectives of this paper are as follows: (1) to present new Rb–Sr and Sm–Nd isotopic data on the Francistown plutonic rocks, (2) to discuss the age, petrogenesis and the source regions of these igneous rocks, and (3) to assess their tectonic implications for the evolution of the Zimbabwe craton.

Geological background

The Zimbabwe craton's lithospheric mantle separated from the asthenospheric mantle at ≥3.8 Ga (Nägler et al. 1997) and the oldest preserved crustal rocks were emplaced between 3565 ± 21 and 3368 ± 11 Ma in the Tokwe nucleus (Fig. 1a, Dodson et al. 1988, 2001; Wilson et al. 1995; Jelsma et al. 1996; Horstwood et al. 1999). Wilson et al. (1978) divided the Archaean Zimbabwe craton into four terrains, largely based on Rb–Sr isotope dates: three generations of granite–greenstone terrains emplaced at ~3.5 Ga, ~2.9 Ga and ~2.7 Ga, and the later Chilimanzi-Razi granite suite emplaced at ~2.6–2.5 Ga. This division has been supported by U–Pb zircon and Sm–Nd dating techniques (Jelsma and Dirks 2002). Each of the granite–greenstone terrains was

Table 1 Collected isotope data for the Francistown Greenstone–Granite terrain

Rock unit	Dating method	Age (Ma)	Reference
Tati Volcanic Group	Rb–Sr whole-rock	2523 ± 33	Van Breemen and Dodson (1972)[a]
Granite (near Francistown)	K–Ar whole-rock	2500 ± 100, 2285 ± 70	Van Breemen and Dodson (1972)[a]
Tonalitic orthogneiss, Vumba granite–greenstone terrain	U–Pb SHRIMP single zircon	2686 ± 6	Bagai et al. (2002)
Granitic gneiss, Vumba granite–greenstone terrain	U–Pb SHRIMP single zircon	2714 + 46/−26	Bagai et al. (2002)
Tonalitic granitoid, Vumba granite–greenstone terrain	U–Pb SHRIMP single zircon	2696 ± 3.5	Bagai et al. (2002)
Granite, Vumba granite–greenstone terrain	U–Pb SHRIMP single zircon	2647 ± 4	Bagai et al. (2002)
Granodiorite gneiss, Mosetse area	U–Pb SHRIMP single zircon	2648 ± 2	Majaule and Davis (1998)
Massive K-feldspar megacrystic monzodiorite, Mosetse area	U–Pb SHRIMP single zircon	2646 ± 2.5	Majaule and Davis (1998)
Fine to medium-grained tonalitic gneiss, Mosetse area	U–Pb SHRIMP single zircon	2710 ± 19	Majaule and Davis (1998)
Medium-grained tonalitic gneiss, Mosetse area	U–Pb SHRIMP single zircon	2648 ± 2.5	Majaule and Davis (1998)

[a]Dates recalculated by Cahen et al. (1984)

started when lavas forming the greenstone belt were deposited, followed by the plutonic bodies including tonalites, trondhjemites, Na–granites and Sanukitoids. The latter, K-rich granite suite consists mainly of monzogranites and granites. The main characteristics of Archaean igneous associations of the Zimbabwe craton in Zimbabwe are listed in (Table 2).

The Zimbabwe craton extends southwest into NE Botswana (Fig. 1a). The Botswana sector consists of Francistown arc complex (McCourt et al. 2004), which is composed of three greenstone belts: the Tati, the Vumba and the Maitengwe Volcanic Groups. These groups are surrounded and locally intruded by complexes of granitoid gneiss and massive granitoid (Fig. 1b, Litherland 1975; Key 1976; Carney et al. 1994; Ranganai et al. 2002). In this study we focus on the plutonic rocks around the Tati greenstone belt.

The Tati granite–greenstone terrain includes the Tati greenstone belt, voluminous granitoids and gabbros, and minor meta-sedimentary rocks (Key 1976; Kampunzu et al. 2003). Nine main and several small intrusive complexes were identified in this terrain (Fig. 2). According to the characteristics of their major and trace element abundances, these complexes were classified into three suites: Trondhjemite–Tonalite–Granite suite (here after TTG suite), Sanukitoid suite and High-K granites. TTG was further classified into two sub-suites: Low Aluminum-TTG (LA-TTG) and High Aluminum-TTG (HA-TTG, Kampunzu et al. 2003). Airport, Tati, South Tati and New Zealand complexes are HA-TTG that intruded the Tati greenstone belt lithologies (Fig. 2, Key 1976). They are mainly gray colored, coarse grained tonalites, trondhjemites and granites. Most samples from these complexes have more than 15% of Al_2O_3 (Kampunzu et al. 2003). Tonalite and trondhjemite are foliated to banded gray gneisses, containing ortho-amphibolitic enclaves. Undeformed whitish-gray to pink, equigranular granites form the rugged hilly terrains at the core of the Tati complex. Sikukwe, Mphoeng and Matsiloje complexes are LA-TTG. Most samples from these regions have less than 15% of Al_2O_3 (Kampunzu et al. 2003). The Matsiloje and Sikukwe complexes are homogenous, coarse-grained gray tonalites and trondhjemites, containing hornblende, biotite, plagioclase and quartz. The Mphoeng complex consists of coarse grained to porphyritic gabbros, tonalites and granodiorites. The gabbro consists of large milky white plagioclase phenocrysts in a dark green coarse-grained matrix of pyroxene, plagioclase, minor hornblende and biotite. The Selkirk complexes and several small intrusives are the Sanukitoid suite, which usually contains more than 7% of MgO (Kampunzu et al. 2003). These include coarse-grained troctolites, gabbros and High-Mg diorites intruding the Tati greenstone belt lithologies. The primary minerals in these rocks include plagioclase, olivine, pyroxene and opaque minerals. The High-K granites usually occur as small stocks and dykes intruding the greenstone belt or other granitoids. The largest outcrop of the High-K granites is the Ramokgwebana complex, which contains large K-feldspar phenocrysts in a coarse-grained matrix of feldspar, biotite, quartz, hornblende, zircon and titanite. Some outcrops of High-K granites are heterogeneous. For example, X-Ray Diffraction (XRD) analysis indicates that sample MK112A contains some actinolite, indicating the influence of lower continental crust enclaves. Sample BR44 is very fractionated with more than 78% SiO_2. There is no schistosity developed in the High-K granites.

Sampling and analysis

Out of 211 samples analysed for major and trace elements compositions in our previous study (Kampunzu et al. 2003), 26 representative samples were selected for

Table 2 Terrains of Zimbabwe craton and their ages

Terrain	Major stratigraphic unit	Major intrusive	U–Pb age (Ga)	Rb–Sr Age (Ga)	Initial ^{87}Sr / ^{86}Sr[b]
Later Granites		Chilimanzi Suite: Chilimanzi, Zimbabwe, Victoria Porphyry	2.519–2.634[d]	2.54[a]–2.66[b]	0.7025–0.7044
The 2,700 Ma Granite–Greenstone terrain	Shamvaian group: sedimentary rocks with minor igneous rocks. Upper Bulawayan group (upper greenstones): felsic, mafic and ultramafic volcanic rocks intercalated with iron formations	Sesombi Suite: Sesombi, Somabula	2.75–2.58[d]	2.54–2.73[b]	0.7008–0.7012
The 2,900 Ma Granite–Greenstone terrain	Lower Bulawayan group (lower greenstones): mafic and ultramafic lavas and minor sedimentary rocks	Chingezi Gneisses, Mashaba tonalite, Gwenoro gneisses	3.10–2.75[d]	2.78–2.97[b]	0.7011–0.7017, 0.7056
The 3,500 Ma Granite–Greenstone terrain	Sebakwian group: ultramafic–mafic volcano –plutonic rocks intercalated with banded iron formations	Mont d'Or formation granite, Mushandike granite, Tokwe Gneisses	3.57–3.37[d]	3.42–3.58[b]	0.7000–0.7017[c]

[a]Frei et al. (1999)
[b]Wilson et al. (1978)
[c]The ^{87}Sr / ^{86}Sr ratio for Mont d'Or formation granite in Selukwe is 0.711
[d]Wilson et al. (1995), Horstwood et al. (1999), Dodson et al. (2001), Jelsma and Dirks (2002)

Table 3 Summary of analytical results of internationally used standards

Standard sample	Number of analysis	Rb (ppm)	Sr (ppm)	$^{87}Sr/^{86}Sr$
SRM607[a]	4	524.3 ± 2.3 (523.90 ± 1.01)	65.42 ± 0.65 (65.485 ± 0.320)	1.20034 ± 0.00022 (1.20039 ± 0.00020)
SRM987[a]	6			0.71025 ± 0.00002 (0.71034 ± 0.00026)

Standard sample	Number of analysis	Sm (ppm)	Nd (ppm)	$^{143}Nd/^{144}Nd$
BCR-1	4	6.631 ± 0.056 (6.59[b])	28.92 ± 0.49 (28.8[b])	0.512626 ± 0.000020 (0.512646[c])
La Jolla	6			0.511846 ± 0.000014 (0.511860[b])

The error listed in this table is two standard deviation (2σ).
[a]Data in bracket are certified values from NIST (National Institute of Standards and Technology)
[b] Recommended values of Govindaraju (1994)
[c] Average value of Wasserburg et al. (1981), Ito et al. (1987) and Thirwall (1991)

Table 4 Comparison of duplicated sample analysis of Sm–Nd isotope composition

Sample	Set	^{147}Sm (n mol/g)	Sm (ppm)	^{144}Nd (n mol/g)	Nd (ppm)	^{147}Sm/^{144}Nd	SD (2 σ)	^{143}Nd/^{144}Nd	SD (2 σ)
TS93	1	2.725	2.732	22.48	13.63	0.1212	0.0024	0.511307	0.000016
TS93	2	2.677	2.684	22.24	13.48	0.1204	0.0024	0.511283	0.000004
TS168A	1	1.131	1.134	9.38	5.69	0.1205	0.0024	0.511332	0.000040
TS168A	2	1.132	1.135	9.35	5.67	0.1212	0.0024	0.511335	0.000005
TS2	1	2.936	2.944	25.90	15.71	0.1134	0.0023	0.511246	0.000014
TS2	2	3.224	3.233	28.37	17.21	0.1137	0.0023	0.511200	0.000006
MK112A	1	1.789	1.794	12.40	7.52	0.1442	0.0029	0.511184	0.000010
MK112A	2	1.892	1.897	13.48	8.17	0.1403	0.0028	0.511171	0.000009

isotopic studies (Fig. 2), consisting of 5 Sanukitoids, 7 LA-TTGs, 4 HA-TTGs and 10 High-K granites.

The analyses were performed at the Institute of Geology and Geophysics, Chinese Academy of Science using standard methods as described elsewhere (e.g. Wasserburg et al. 1981; Kagami et al. 1989). Briefly, about 100 mg of rock powder was digested by a mixture of $HClO_4$ and HF acids. Rb–Sr–REE were separated using the resin of AG50W-12 and Sm–Nd were separated using the resin of P507. Isotope compositions were measured by a Finnigan MAT 262 Thermal Ionisation Mass Spectrometer (TIMS) using multicollector mode. Metal ions were analyzed and the total blanks for Rb, Sr, Sm and Nd are about 80, 60, 40, and 50 pg, respectively. The measured Sr isotope data was normalized to the ratio $^{86}Sr/^{88}Sr = 0.1194$ and the measured $^{143}Nd/^{144}Nd$ ratios were normalized using the ratio $^{146}Nd/^{144}Nd = 0.7219$. Nd and Sr isotopic ratios are uncorrected beyond mass fractionation. The concentrations of Rb, Sr, Sm and Nd were analyzed by isotope dilution method.

Four internationally used standards were analyzed routinely in the lab for quality control purposes and the analytical results are summarized in Table 3. The whole-rock standards SRM607 and BCR-1 were used to monitor the chemical procedure; the pure chemical standards SRM987 and La Jolla were used to monitor the instrument states. Table 3 indicates that the accuracy were better than 0.1% for Rb and Sr concentrations and better than 0.7% for Sm and Nd. The standard deviations (2σ) for the measurements of $^{87}Rb/^{86}Sr$ and $^{143}Nd/^{144}Nd$ are between 0.003 and 0.03%. Table 3 indicates that the average values of Rb, Sr, Sm and Nd concentrations and $^{87}Sr/^{86}Sr$ and $^{143}Nd/^{144}Nd$ ratios obtained are in the range of the recommended values if 2σ uncertainties are considered, and is similar to the

Table 5 Rb–Sr isotope composition of Francistown plutonic rocks

Sample	Rock type[a]	Rb (ppm)	Sr (ppm)	$^{87}Rb/^{86}Sr$	$^{87}Sr/^{86}Sr$	SD[b] (2σ)
MK125	1	0.4362	8.608	0.1468	0.716337	0.000009
MK32	1	89.59	172.9	1.506	0.749679	0.000007
NN58	1	0.1132	313.1	0.001	0.703041	0.000009
TS169	1	2.507	207.4	0.03499	0.711096	0.000025
TS93	1	1.335	87.01	0.04441	0.704707	0.000011
NN82B	2	56.16	472.5	0.3443	0.714419	0.000008
TS168A	2	56.4	356.5	0.4584	0.718074	0.000009
TS168B	2	52.81	218.3	0.7015	0.726735	0.000009
TS2	2	99.71	197	1.472	0.75864	0.00011
BR24A	3	46.35	186.4	0.7216	0.733659	0.000011
MK43A	3	100.3	109	2.688	0.800784	0.000011
MK43B	3	51.04	185.7	0.7976	0.73535	0.000100
TS56	3	1.38	129.9	0.0307	0.70296	0.00010
TS70	3	46.45	79	1.712	0.767341	0.000013
TS82	3	82.09	131.7	1.816	0.772191	0.000011
TS94	3	97.29	112.1	2.531	0.784373	0.000010
BR24B	4	127.6	102.7	3.639	0.831313	0.000010
BR44	4	127.9	34.13	11.28	1.111762	0.000017
MK112A	4	306.4	102.3	8.924	1.010558	0.000011
MK112B	4	283.3	103.6	8.134	0.992073	0.000012
MK112C	4	184.6	177	3.049	0.813682	0.000010
MK19	4	133.3	139.6	2.785	0.792755	0.000012
MK31B	4	196.1	104.8	5.513	0.889554	0.000012
NN23B	4	125.9	236.2	1.551	0.764523	0.000009
BR110	4	1.576	16.9	0.2701	0.713682	0.000012
BR88	4	4.101	16.9	0.7036	0.729219	0.000014

[a]Rock type: *1*, Sanukitoid suite; *2*, HA TTG subsuite; *3*, LA TTG subsuite; *4*, High-K granites
[b]SD (standard deviation) is the measurement error of each sample

Table 6 Sm–Nd isotope compositions, model ages and epsilon values of Francistown plutonic rocks

Sample	Rock type[a]	Sm (ppm)	Nd (ppm)	$^{147}Sm/^{144}Nd$	$^{143}Nd/^{144}Nd$	SD[b] (2 σ)	T-DM model age[c]	Nd epsilon rock, t [d]	Nd epsilon rock, t [e]	Nd epsilon rock, today [f]
MK125	1	1.652	7.494	0.1333	0.511615	0.000009	2.6	2.1	1.7	−20
MK32	1	2.83	13.74	0.1246	0.511320	0.000005	2.8	−0.7	−1.1	−26
NN58	1	3.585	18.27	0.1187	0.511198	0.000005	2.8	−1.0	−1.5	−28
TS169	1	3.973	17.21	0.1396	0.511620	0.000008	2.7	0.0	−0.4	−20
TS93	1	2.708	13.56	0.1208	0.511295	0.000010	2.7	0.2	−0.3	−26
Average 1	1						2.7	0.1	−0.3	−24
NN82B	2	0.8468	4.493	0.114	0.511263	0.000006	2.6	1.9	1.4	−27
TS168A	2	1.135	5.68	0.1209	0.511334	0.000023	2.7	0.9	0.4	−25
TS168B	2	1.627	9.333	0.1054	0.511129	0.000015	2.6	2.3	1.7	−29
TS2	2	3.089	16.46	0.1136	0.511223	0.000010	2.6	1.3	0.7	−28
Average 2	2						2.6	1.6	1.1	−27
BR24A	3	1.683	9.501	0.1071	0.511027	0.000010	2.8	−0.3	−0.9	−31
MK43A	3	4.307	24.95	0.1044	0.510991	0.000011	2.7	−0.1	−0.7	−32
MK43B	3	2.001	11.35	0.1067	0.511017	0.000012	2.8	−0.3	−0.9	−32
TS56	3	5.778	33.69	0.1037	0.510957	0.000007	2.8	−0.5	−1.1	−33
TS70	3	7.535	36.95	0.1235	0.511276	0.000012	2.8	−1.1	−1.6	−27
TS82	3	1.827	9.424	0.1172	0.511302	0.000009	2.6	1.6	1.1	−26
TS94	3	5.737	29.05	0.1194	0.511225	0.000008	2.8	−0.7	−1.2	−28
Average 3	3						2.8	−0.2	−0.8	−30
Average 4	2+3						2.7	0.5	−0.1	−29
Average 5	1+2+3						2.7	0.4	−0.2	−27
BR24B	4	3.287	18.33	0.1084	0.511073	0.000009	2.7		−0.4	−31
BR44	4	0.3578	3.561	0.0608	0.510215	0.000011	2.7		−0.9	−47
MK112A	4	1.846	7.85	0.1423	0.511178	0.000010	3.7		−10.0	−28
MK112B	4	6.29	35.24	0.108	0.511018	0.000010	2.8		−1.4	−32
MK112C	4	8.856	53.6	0.0999	0.510894	0.000007	2.8		−1.0	−34
MK19	4	0.7606	3.285	0.14	0.511532	0.000011	2.9		−2.3	−22
MK31B	4	3.116	8.127	0.2319	0.513199	0.000011	1.3		−1.1	11
NN23B	4	1.741	10.7	0.0984	0.510743	0.000013	2.9		−3.5	−37
BR110	4	4.332	22.24	0.1178	0.511219	0.000007	2.8		−0.8	−28
BR88	4	1.717	7.754	0.134	0.511494	0.000014	2.8		−0.9	−22
Average 6	4						2.8		−1.4	−31

Average 1, Average of Sanukitoid suite; *Average 2*, Average of HA-TTG subsuite; *Average3*, Average of LA-TTG subsuite; *Average 4*, Average of TTG suite; *Average 5*, Average of Sanukitoid and TTG suite; *Average 6*, Average of High-K granites, Sample MK112A and MK31B are not included

[a]Rock type: *1*, Sanukitoid suite; *2*, HA TTG subsuite; *3*, LA TTG subsuite; *4*, High-K granites

[b]SD (Standard deviation) is measurement error of each sample

[c](143Nd/144Nd)DM, today = 0.513114, (147Sm/144Nd)DM, today = 0.222, (Michart et al. 1985)

[d]Nd epsilon values for individual rocks at the time of formation of Sanukitoid and TTG suites, $t = 2.7$ Ga

[e]Nd epsilon values for individual rocks at the time of formation of High-K granites, $t = 2.65$ Ga

[f]Nd epsilon values for individual rocks at the present day

measured values in some other laboratories (e.g. Liu et al. 2004). Because the internal measurement errors of samples are smaller than the 2σ external reproducibilities of standards, the 2σ external reproducibilities represent the estimates of sample errors (Editorial 2003). For $^{87}Rb/^{86}Sr$ and $^{147}Sm/^{144}Nd$ ratios, the errors are 2%; for $^{87}Sr/^{86}Sr$, the error is 0.03% and for $^{143}Nd/^{144}Nd$ ratio, the error is 0.004%.

In order to define the precision of the data, four samples were analyzed twice and the results are listed in Table 4. The individual measurements for duplicated sample TS168A and MK112A are within two standard deviations of their original analyses. Although the difference between the duplicate analyses and original analyses for sample TS93 and TS2 are slightly larger than their measurement errors (2 standard deviations), they are within the 2σ external reproducibilities. This means that the precisions of analyses are acceptable. The analytical results of the Rb–Sr and Sm–Nd isotope compositions are listed in Tables 5 and 6, respectively. For samples with duplicate analyses, the average was listed.

Results and discussion

The analytical results of the Rb–Sr and Sm–Nd isotope compositions are plotted in Figs. 3 and 4, respectively. The isochron dates and initial ratios are calculated using Isoplot Version 2.8 (Ludwig 2001).

Rb–Sr isotope systematics

The Sanukitoid, the TTG and the High-K granite samples yield isochron dates 1.986 ± 0.780, 2.437 ± 0.230, and 2.446 ± 0.095 Ga, and the initial $^{87}Sr/^{86}Sr$ ratios 0.7071 ± 0.0077, 0.7043 ± 0.0049 and 0.7028 ± 0.0076,

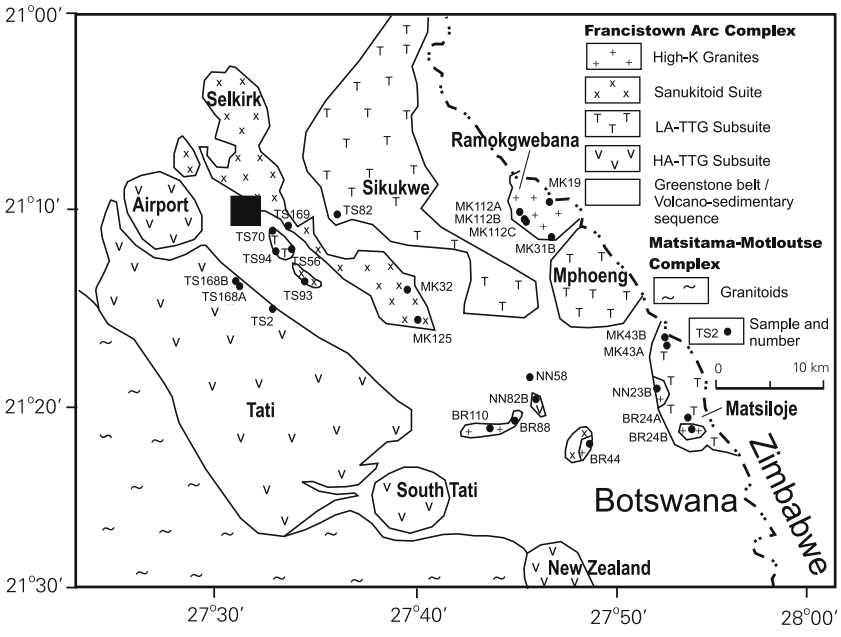

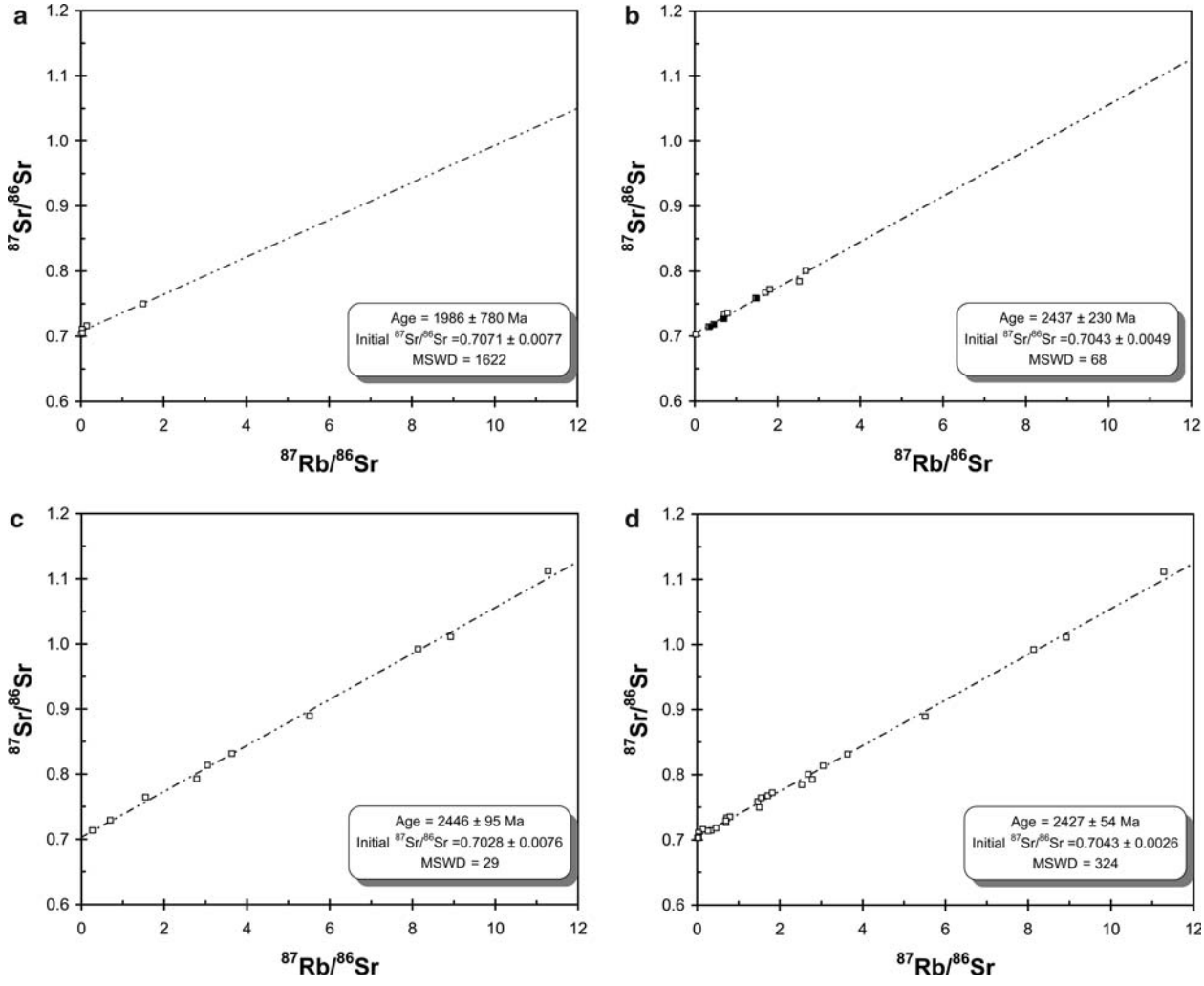

Fig. 2 Geological map of the Tati Granite–Greenstone Terrain of the Francistown arc complex. The *black square* is Francistown City. The names of the nine major intrusive complexes are labeled in or beside their exposure areas. Sample NN58 was collected from an intrusion of Sanukitoid, which is too small to be shown in this map

Fig. 3 Whole rock Rb–Sr isochron of the Francistown granitoids. **a** Sanukitoid suite; **b** TTG suite; **c** High-K granites; **d** all samples. The *dashed line* represents the isochron. The error is (2σ) 2% for $^{87}Rb/^{86}Sr$ and 0.03% for $^{87}Sr/^{86}Sr$. *Each square* corresponds to one sample. For the TTG suite, the *solid squares* represent HA-TTG, the *open squares* LA-TTG

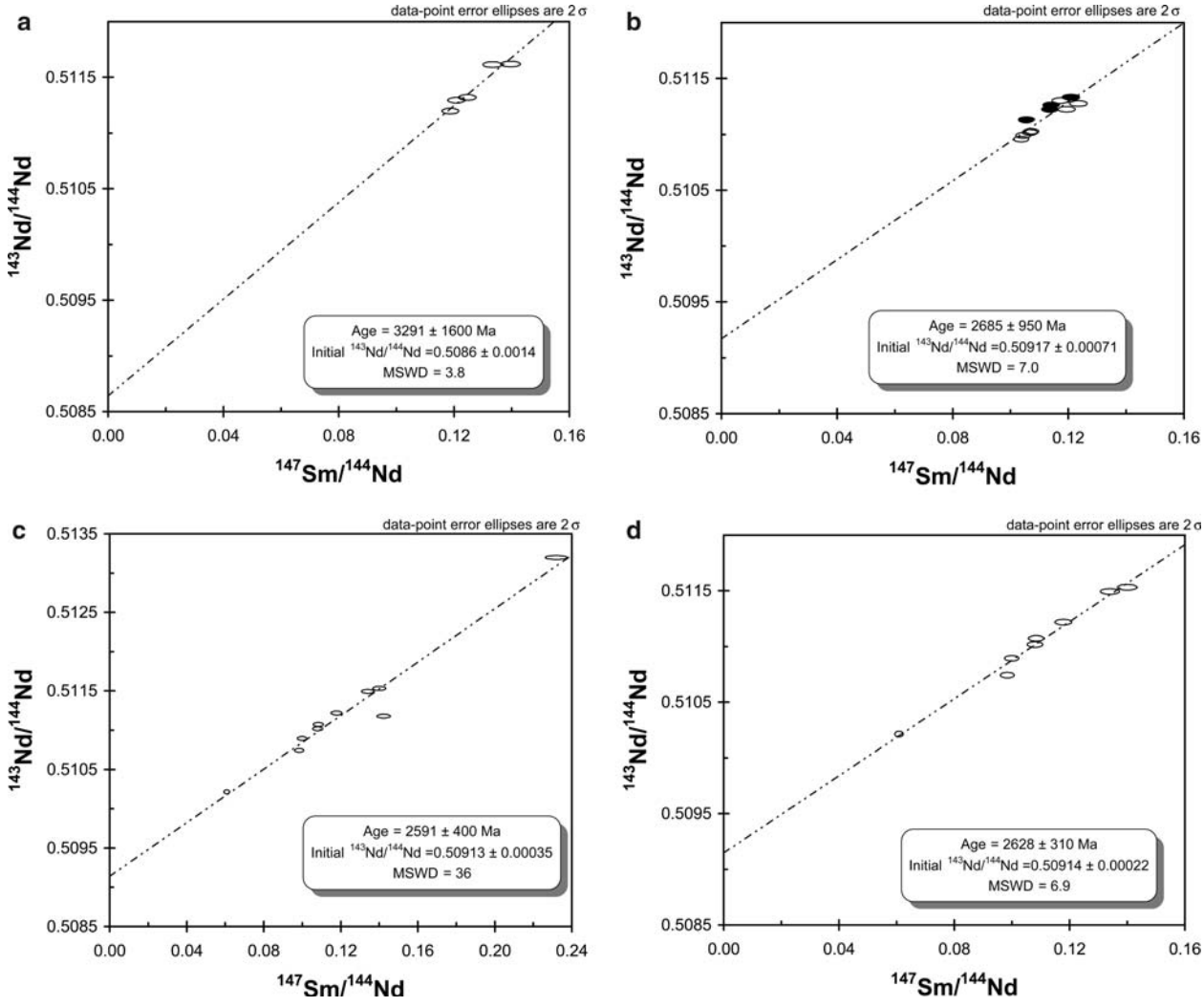

Fig. 4 Whole rock Sm–Nd isochron of the Francistown granitoids. **a** Sanukitoid suite; **b** TTG suite; **c** High-K granites; **d** High-K granites (samples MK112A and MK31B are excluded). The *dashed line* represents the isochron. The error (2σ) is 2% for $^{147}Sm/^{144}Nd$ and 0.004% for $^{143}Nd/^{144}Nd$. For the TTG suite, the solid error ellipses represent the HA-TTG and the open error ellipses the LA-TTG

respectively, as shown in Figs. 3a, b and c. In the margins of error, there are no significant differences in the isochron dates and the initial $^{87}Sr/^{86}Sr$ ratios calculated from the different rock types. In order to compare with previous data, the 26 samples were plotted in one diagram, yield an isochron date of 2.427 ± 0.054 Ga and an initial $^{87}Sr/^{86}Sr$ ratio of 0.7043 ± 0.0026 (Fig. 3d). Although the Rb–Sr isochron date is close to the previously reported date of 2523 ± 33 Ma (Table 1, Van Breeman and Dodson 1972), it is much younger than the Rb–Sr date of Neoarchaean TTG in the Zimbabwe craton and the U–Pb SHRIMP zircon igneous crystallization age (Table 2). Furthermore, this initial $^{87}Sr/^{86}Sr$ ratio is larger than that at most other sites in the Zimbabwe craton (Table 2). These Rb–Sr isochron ages have large errors and mean squares of weighted deviated (MSWD) values, as shown in Fig. 3, and are also younger than the dates of the same rocks from the Sm–Nd method (see below). These factors indicate that the Rb–Sr isochron dates are likely not to be representative of the crystallization ages, indicating that a thermo-tectonic event and/or an alteration that partly reset the Sr isotope system have occurred. The widespread migmatization in the TTG, the varying degrees of sericitization and the chloritization in all rock types indicate that partial melting and fluid circulation have played an important role for this resetting. Therefore, the Rb–Sr isotope data can only provide the lowest boundary on the age of the Francistown plutonic rocks. This thermo-tectonic event presumably was stronger along the south-western margin of the Zimbabwe craton but did not significantly reset the Rb–Sr isotope system of the centre of the craton where Wilson et al. (1978) successfully measured the ages of the four terrains using the Rb–Sr isotope dating methods.

Sm–Nd isotope systematics

The $^{143}Nd/^{144}Nd$ and $^{147}Sm/^{144}Nd$ ratios for the Sanukitoid, the TTG and the High-K granite samples yield isochron dates of 3.29 ± 1.60, 2.69 ± 0.95 and 2.59 ± 0.40 Ga, respectively (Fig. 4a–c). Sample MK112A is affected by the old lower continental crust (see above) and its Nd isotope compositions are significantly different from other samples (Fig. 4c). Sample MK31B was collected near the boundary to a greenstone belt. It has a high $^{147}Sm/^{143}Nd$ ratio (0.2319), similar to that of oceanic crust (MORB) or depleted mantle (Rollinson 1993). This indicates the influence of the greenstone belt. Thus, these two samples are excluded from the discussion of Nd isotope of High-K granites. The remaining samples yield an isochron date of 2.63 ± 0.31 Ga for the High-K granites, as shown in Fig. 4d. Figure 4 shows that the isotope data are scattered in the $^{143}Nd/^{144}Nd$ versus $^{147}Sm/^{144}Nd$ plots and the calculated isochron dates have large errors. Since all the duplicates agree with original analysis, as shown in Table 3, we cannot completely attribute these deviations to errors of analyses. Brook et al. (1972) suggested that if the MSWD is 2.5 or less, the origin of the scatter on an isochron is analytical, otherwise, it is geological. In this case, the MSWD for Sanukitoid, TTG and High-K granites are 3.8, 7.0 and 6.9, respectively (Fig. 4a, b, d), implying that the errors of the isochron dates are geological. There are three major possibilities for the large error reported here:

1. Fractionation of Sm is too small among different samples;
2. Different degrees of contamination of the crust;
3. Neodymium isotope composition of the source is heterogeneous.

The large errors in the estimated Sm–Nd isotope isochron ages indicate that these dates are still poorly constrained. For further discussion, more precise ages of these three suites are necessary. Therefore, here we adopt precise ages for the same rock types and measured in the adjacent area as references. For this purpose, U–Pb SHRIMP single zircon ages measured in Vumba granite–greenstone terrain (Fig. 1b, Bagai et al. 2002) were chosen, because:

1. Tati and Vumba terranes are adjacent to each other; and both terranes constitute vast portion of the Francistown arc complex (Fig. 1b).
2. Lithologic characters of granitoids in Tati and Vumba area are similar.
3. The felsic magmatism in Vumba occurred between ca. 2696 ± 3.5 and 2647 ± 4 Ma (Bagai et al. 2002). This age range is similar to that of 2710 ± 9–2646 ± 3 Ma recorded by Majaule and Davis (1998) in the adjacent Mosetse area which is also part of the Francistown arc complex (Fig. 1b; Table 1). Therefore, it is reasonable to assume that the granitoids in the Tati area are likely to have similar ages.
4. The model ages of TTG (2.6 Ga) and Sanukitoid suites (2.6 Ga, see below) are close to the U–Pb Single zircon ages recorded in the Vumba area which is compatible with the adoption of U–Pb SHRIMP dates.

U–Pb SHRIMP single zircon ages indicate that most felsic plutons, from G1 to G4 (i.e. Sanukitoid and TTG suite in this study) in Vumba area crystallized between 2.696 ± 4 and 2.686 ± 6 Ga, except for G5 (High-K granites in this study) which crystallized 2.647 ± 4 Ga ago (Bagai et al. 2002). Therefore, the single zircon age of 2.7 Ga is used as a reference for TTG and Sanukitoid suites and the age of 2.65 Ga is used for the High-K granites.

ε_{Nd} values and magma source characteristics

In order to quantitatively evaluate the Nd isotope composition of the source of Francistown plutonic rocks, the ε_{Nd} values of individual samples at the time of formation of Sanukitoid and TTG suites (ε^t_{Nd}, at 2.7 Ga) and High-K granites (at 2.65 Ga) and the ε_{Nd} values at the present day (ε^{today}_{Nd}) were calculated (Table 6) according to DePaolo and Wasserburg (1976).

The highest ε^t_{Nd} values of Sanukitoids and TTG are $+2.1$ and $+2.3$, respectively (Table 6). The positive ε^t_{Nd} values suggest that TTG and Sanukitoid suites were derived from a source, which had higher $^{143}Nd/^{144}Nd$ ratio than CHUR. This source could be the depleted upper mantle or an oceanic crust, which has a higher Sm/Nd ratio and therefore a higher concentration of the radiogenic isotope ^{143}Nd. If the oceanic crust is derived from the depleted mantle similar to oceanic crust along the mid-ocean ridges, and is very young (the change of the $^{143}Nd/^{144}Nd$ ratio and the ε_{Nd} values is small), the magma derived from partial melting of such a crust have positive ε_{Nd} values, which is close to that of depleted mantle. It is widely believed that the time between the creation and subduction of oceanic plate was significantly shorter in the Archaean (~20 Ma) than it is today (e.g. Shirey and Hanson 1986; McCulloch and Bennett 1993; Kamber et al. 2002). This would imply that melting of a young subducting oceanic crust could generate magmas with positive ε^t_{Nd} values, similar to that of the depleted mantle. Therefore a subducting oceanic crust is also a possible source for igneous rocks with positive ε^t_{Nd} values.

The average ε^t_{Nd}, ε^{today}_{Nd} values and the highest and lowest ε^t_{Nd} values of different suites of Francistown Granitoids are plotted in Fig. 5, together with that of the depleted mantle from two references. DePaolo (1981a, b) studied the variation of the ε_{Nd} values of depleted mantle and derived the relationship between geological age and the ε_{Nd} value ($\varepsilon_{Nd} = 0.25t^2 - 3t + 8.5$, where t is the time before the present in Ga). When $t = 2.7$ Ga, this ε_{Nd} value equals to $+2.17$. Nägler and Kramers (1998) critically reviewed compilation of Nd initial isotope ratios of Precambrian and lunar rocks,

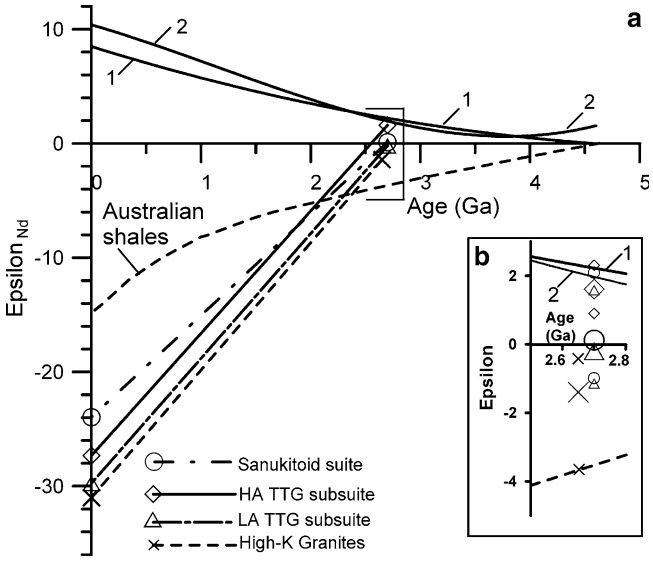

Fig. 5 ε_{Nd} value variations for Francistown plutonic rocks. **a** is the variation of the average ε^t_{Nd} values of different suites of Francistown plutonic rocks. The *two solid lines* indicate the evolution of the Nd isotopes of the depleted upper mantle. *Line 1* is from DePaolo (1981a, b); *line 2* is from Nägler and Kramers (1998). The *dashed curve* is for Australian shales from Allègre and Rousseau (1984) and is thought to approximate to the evolution of average continental crust through time (Rollinson, 1993) **b** is the enlargement of the *rectangle area* in **a**. The *smaller symbols* represent the highest or lowest ε^t_{Nd} values, the *larger symbols* represent the average of ε^t_{Nd} values of each suite of plutonic rocks

and proposed a new equation to describe the evolution of the Nd isotopes of the depleted upper mantle ($\varepsilon_{Nd}[T]_{sample} = 0.164T^3 - 0.566T^2 - 2.79T + 10.4$, where T is the time before the present in Ga). When $T = 2.7$ Ga, the calculated ε_{Nd} value of the depleted mantle is +1.90. These values are very similar to the highest ε^t_{Nd} value of the Sanukitoid suite (sample MK125, +2.1), suggesting that the source of Sanukitoids was the depleted upper mantle. The ε^t_{Nd} values of other four Sanukitoid samples are lower than that of sample MK125, pointing to a contamination by an older continental crust. The major and trace element characteristics (e.g. high $Mg^{\#}$ and high transition metal contents) also suggest that the Sanukitoid suite was generated in the upper mantle (Kampunzu et al. 2003). This conclusion is in good agreement with the general opinion regarding the formation of Sanukitoids in Archaean cratons (e.g. Shirey and Hanson 1984; Stern et al. 1989; Stern and Hanson 1991), that is further supported by experimental studies (e.g. Tatsumi 1981).

The highest ε^t_{Nd} value of TTG suite (+2.3, sample TS168B) is also close to the calculated depleted mantle ε_{Nd} value. In the light of the characteristics of major and trace element abundances of these rocks (e.g. $Mg^{\#} < 0.5$, low Ni and Cr contents), Kampunzu et al. (2003) concluded that both HA- and LA-TTG sub-suites were formed by partial melting of mafic rocks, but not mantle rocks. This conclusion is in good agreement with opinions of other workers (e.g. Arth and Hanson 1972, 1975; Hanson and Goldich 1972; Whalen et al. 2002). However, there is a divergence of opinion on the processes involved during the petrogenesis of the TTGs. Some geologists (e.g. Petford and Atherton 1996) suggested that TTG magmas form during partial melting of mafic rocks underplated within the crust. Others (e.g. Drummond and Defant 1990) attribute TTG genesis to partial melting of mafic rocks within a subducting oceanic slab. The HA-TTG sub-suite of Francistown is characterized by the low concentrations of Y, the strong depletion of HREE in the chondrite-normalized diagram, the overall high concentration of Sr and the strong Nb negative anomalies (Kampunzu et al. 2003), requiring the presence of garnet and amphibole and no plagioclase in the melt residue. Rushmer (1991) pointed out that amphibole is a stable phase up to 18 kb at 950°C and therefore it could be among residual minerals during dehydration melting of the oceanic crust. Some experimental studies (e.g. Rapp et al. 1991) showed that, during dehydration melting of mafic rocks at about 700–1,000°C and high pressure (≥1.5 GPa), the trondhjemitic melt generated has Al-rich composition and the melt residue is plagioclase-free and rich in amphibole and garnet. Therefore, Kampunzu et al. (2003) concluded that HA-TTGs were derived from partial melting of a shallow subducting oceanic plate. Different from HA-TTGs, LA-TTGs have lower Al_2O_3 (usually ≤ 15%) and Sr concentrations, higher LREE concentrations, and significant Eu negative anomalies. Their chemical composition is similar to that of experimental melts produced from garnet amphibolite at pressures between 8 and 15 kb (Rapp 1997; Wyllie et al. 1997). Thus, Kampunzu (2003) suggested that LA-TTGs were generated from partial melting of mafic igneous rocks converted into garnet amphibolite within the lower continental crust. The Nd isotope data supports the first conclusion (HA-TTGs were derived from partial melting of a subducting oceanic plate), but does not support the second one (LA-TTGs were generated from garnet amphibolite within the lower continental crust), because the products of partial melting of a continental crust usually have negative ε_{Nd} values (Rollinson 1993). The dashed curve in Fig. 5 is for Australian shales from Allègre and Rousseau (1984) and is thought to approximate the evolution of average continental crust through time. From this curve we found that 2.7 Ga ago, the ε_{Nd} value is about −3.8. However, most LA-TTG samples have ε_{Nd} values, which are positive or close to zero (Table 6). Table 6 indicates that the highest ε_{Nd} values for LA-TTG (+1.6, sample TS82) and HA-TTG (+2.3) are quite close to each other. The major and trace element abundances of HA- and LA-TTGs also have some similarities, such as high Na_2O, Na_2O/K_2O and alumina saturation index (ASI = molecular ratio $Al_2O_3/(CaO + Na_2O + K_2O)$, Kampunzu et al. 2003). These similarities suggest that HA- and LA-TTGs formed from the same source, the young oceanic plate. This conclusion agrees with findings presented in previous studies (e.g. Martin 1993).

We will now investigate the possible cause for the differences between LA-TTG and HA-TTG, especially, for

the differences between the ε^t_{Nd} values of LA-TTG (−1.1 to +1.6, average −0.20) and HA-TTG (+0.9 to +2.3, average +1.6, Table 6). In order to study the relationship between LA- and HA-TTG, the SiO_2 and Al_2O_3 concentrations and the ε^t_{Nd} values of the eleven TTG suite samples are listed in Table 7 and plotted in Fig. 6. Figure 6a suggests that Al_2O_3 concentration of TTG decreases as the SiO_2 concentration increases. This correlation is recognized in most TTG world-wide (Barker 1979). The increase of SiO_2 (or the decrease of Al_2O_3) can be explained by the removal of plagioclase through fractionation crystallization (Barker et al. 1979). Figure 6b shows that as Al_2O_3 concentration decreases, the ε^t_{Nd} values also decreases. Similar correlation can also be found in trace elements. The Eu negative anomalies (Eu*–Eu, where Eu* is an interpolated value for Eu based upon the concentrations of Sm and Gd) and the Sr concentrations in TTG suite are listed in Table 7 and plotted in Fig. 7 against their ε^t_{Nd} values. The negative Eu anomaly is formed mainly by removing the plagioclase during fractionation crystallization (e.g. Rollinson 1993). Sr is a strong compatible element for plagioclase and therefore its concentration will decrease if plagioclase is removed from the magma (e.g. Rollinson 1993). Figure 7 shows the correlation between negative Eu anomaly, Sr concentration and the ε^t_{Nd} values. However, it is well known that fractionation crystallization does not change isotope composition of Sm and Nd and the decrease of the ε^t_{Nd} values usually is caused by contamination of materials from the continental crust (e.g. Faure 1986; Dickin 1995). Thus the correlations between the Sr, Al_2O_3, Eu negative anomalies and the ε^t_{Nd} values indicate that the parental magma of the TTG suite underwent crystal fractionation coupled with crustal contamination en route to the surface and/or in crustal magma chambers. Therefore, the LA-TTG is the product of the fractionation crystallization and crustal contamination of HA-TTG.

The ε^t_{Nd} values of the High-K granite suite are from −3.5 to −0.4, with an average of −1.4 (sample MK112A and MK31B are excluded, see above). The negative ε^t_{Nd} values of High-K granites indicate that they were not derived from the depleted upper mantle or ocean plate, but rather, from a source with a $^{143}Nd/^{144}Nd$ ratio lower than that of CHUR, pointing to an old continental crust (e.g. Rollinson 1993; Dickin 1995). This is supported by the existence of ~3.5–3.6 Ga rock assemblages in the Zimbabwe craton (Dodson et al. 1988, 2001; Wilson et al. 1995; Jelsma et al. 1996; Nägler et al. 1997; Horstwood et al. 1999). Using the curve of Australian shales (Allègre and Rousseau 1984) we may find that at the time of the formation of High-K granites, 2.65 Ga ago, the ε_{Nd} value of the average continental crust was about −3.8. Kampunzu et al. (2003) suggested that High-K granites were formed by partial melting of TTG in the crust. The ε_{Nd} values of LA-TTG of the Francistown area are between +1.1 and −1.7, with an average of −0.8 (Table 6). These ε_{Nd} values are close to that of the High-K granites (Table 6). Thus, the LA-TTG and early Archaean TTG in the lower continental crust are the sources of the High-K granites.

Estimation of the contamination by the continental crust

In order to estimate the percentage of continental crust mixed into the Sanukitoid and TTG magmas, we assume that the continental crust had Sm–Nd isotope composition similar to that of the early Archaean gneisses and plutons in Zimbabwe craton. Taylor et al. (1991) listed the Sm–Nd isotope compositions of some early Archaean samples in Zimbabwe craton: Tokwe gneiss (3.56–3.60 Ga), Shabani gneiss (3.24–3.46 Ga), Mont d'Or granite (3.64–3.67 Ga) and Mushandike granite (3.54 Ga, see Table 2). The averages of these early Archaean samples are: Nd = 23.775 ppm, $^{147}Sm/^{144}Nd = 0.1016$, and $^{143}Nd/^{144}Nd = 0.510471$. The ε^t_{Nd} value of the continental crust at the time of the formation of Sanukitoid and TTG suites (2.7 Ga) was −9.29. After the contamination of the continental crust, the ε^t_{Nd} values of the Sanukitoid/TTG magma will decrease. The ε^t_{Nd} value of the mixture of the magma can be calculated using the following equation (Faure 1986):

$$\varepsilon^X_M = \frac{\varepsilon^X_A X_A f + \varepsilon^X_B X_B (1-f)}{X_A f + X_B (1-f)}, \quad (1)$$

Table 7 Epsilon values, major and trace element concentrations of the TTG suite

Sample	Rock type[a]	Nd epsilon rock, t[b]	SiO_2 (%)	Al_2O_3 (%)	Eu*–Eu (ppm)	Sr (ppm)
NN82B	2	1.9	70.00	16.68	0.75	501
TS168A	2	0.9	71.21	15.07	0.80	402
TS168B	2	2.3	71.61	15.30	1.70	223
TS2	2	1.3	68.10	15.86	2.85	228
BR24A	3	−0.3	74.50	13.86	1.10	196
MK43A	3	−0.1	75.22	13.53	3.70	120
MK43B	3	−0.3	76.00	14.20	1.40	184
TS56	3	−0.5	67.41	14.20	5.12	130
TS70	3	−1.1	74.46	10.94	5.05	75
TS82	3	1.6	74.39	13.53	1.30	128
TS94	3	−0.7	77.92	11.23	4.25	112

[a]Rock type: *2*, HA-TTG subsuite; *3*, LA-TTG subsuite
[b]Nd epsilon values for individual rocks at their time of formation

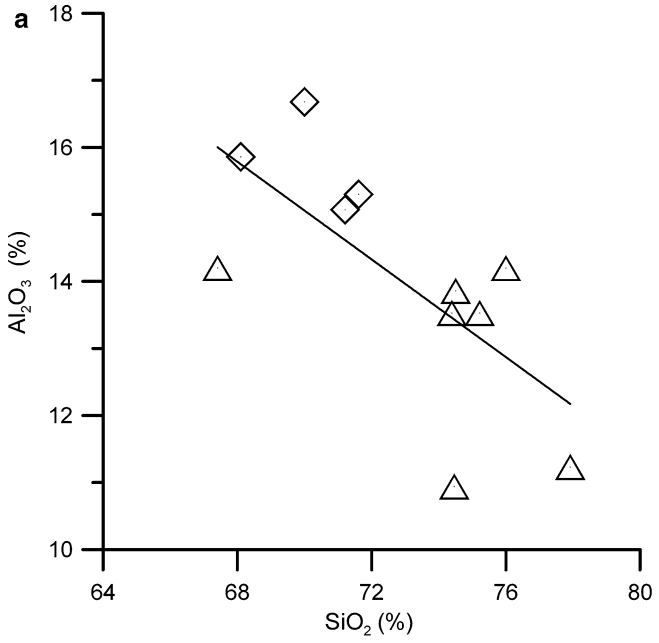

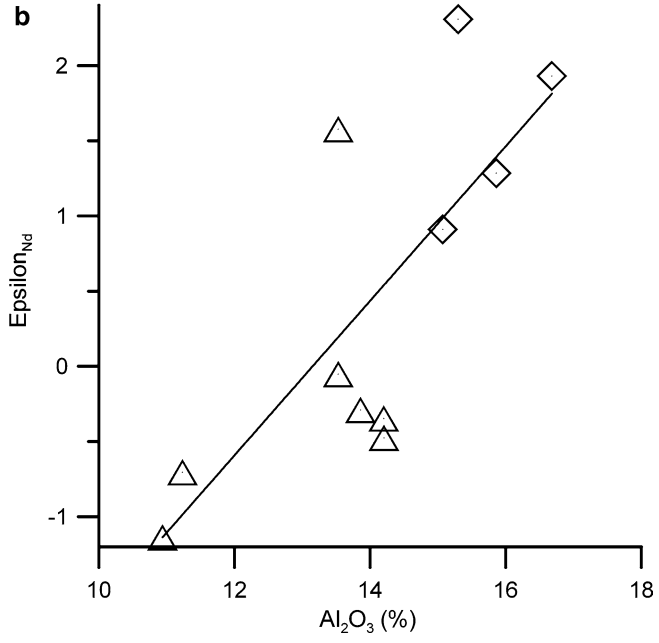

Fig. 6 Correlation of major elements and the ε^t_{Nd} values for the TTG suite. **a** SiO_2 vs. Al_2O_3; **b** Al_2O_3 vs. ε^t_{Nd}. *Diamond symbols* are HA-TTG, *triangle symbols* are LA-TTG. The *straight line* is the fit of the data

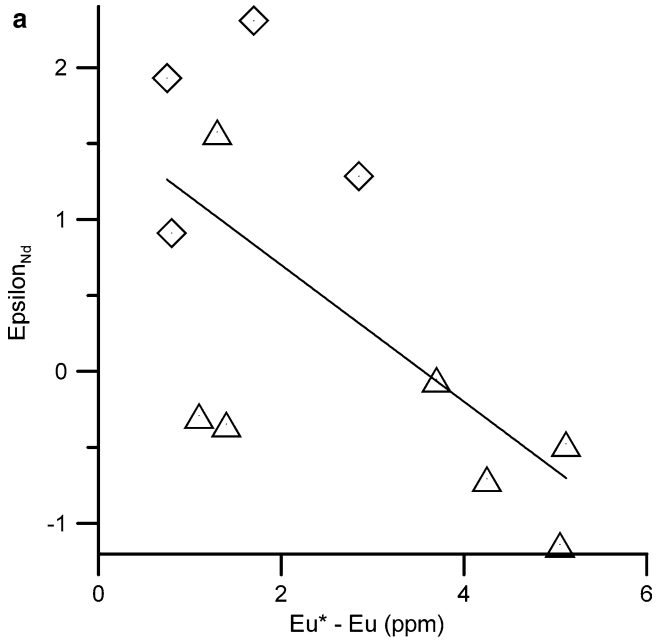

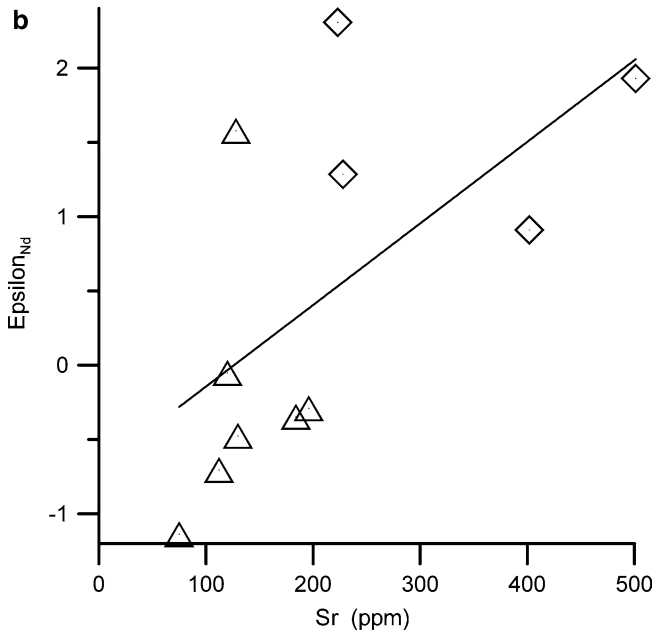

Fig. 7 Correlation of Eu anomalies and Sr concentrations with the ε^t_{Nd} values of TTG suite. **a** ε^t_{Nd} values vs. Eu*–Eu; **b** ε^t_{Nd} values vs. Sr. *Diamond symbols* are HA-TTG, *triangle symbols* are LA-TTG. The *straight line* is the fit of the data

where X_A, X_B are concentrations of element X (here is Nd) in continental crust and the original Sanukitoid/TTG magma respectively; ε^X_A, ε^X_B, and ε^X_M are the ε^t_{Nd} values in continental crust, the original Sanukitoid/TTG magma and the mixture of Sanukitoid/TTG magma and contaminating continental crust, respectively, f is the weight fraction of continental crust in the mixture. The f value equals to:

$$f = \frac{(\varepsilon^X_M - \varepsilon^X_B)X_B}{(\varepsilon^X_M - \varepsilon^X_B)X_B - (\varepsilon^X_M - \varepsilon^X_A)X_A}. \quad (2)$$

We may assume that the sample with the highest ε^t_{Nd} value represents the original Nd composition without continental contamination (MK125 for Sanukitoid

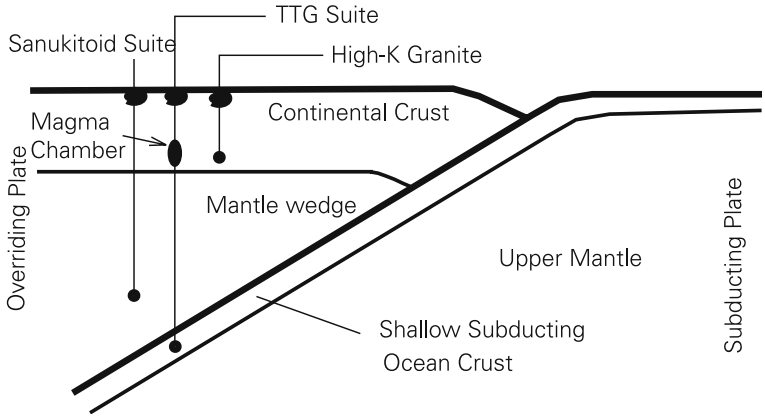

Fig. 8 The model for the formation of Francistown plutonic rocks. Vertical and horizontal scales are different. The TTG suite was formed by the partial melting of a subducting ocean plate 2.7 Ga ago. Its parental magma underwent crystallization fractionation coupled with crustal contamination en route to the surface and/or in the crustal magma chambers. The Sanukitoid suite was formed by the partial melting of upper mantle at about the same time. High-K granites were formed by partial melting of the lower continental crust 2.65 Ga ago

suite, Nd = 7.494 ppm, $\varepsilon^t_{Nd} = 2.1$, sample TS168B for TTG suite, Nd = 9.333 ppm, $\varepsilon^t_{Nd} = 2.3$) and the sample with the lowest ε^t_{Nd} value represent the Nd isotope composition with the maximum continental contamination (sample NN58, $\varepsilon^t_{Nd} = -1.0$ for Sanukitoid suite, sample TS70, $\varepsilon^t_{Nd} = -1.1$ for TTG suite). Using Eq. 2, we can calculate the maximum continental contamination. The maximum weight fraction of contaminating continental crust for Sanukitoid suite is 10%, for TTG suite is 14%.

Model ages

The depleted mantle model Nd ages (T_{DM}) listed in Table 6 lead to the following observations:

1. The sample with least continental contamination for Sanukitoid (MK125) and TTG (TS168B) suites yield a model age of 2.6 Ga, which is similar to their age of crystallization, 2.7 Ga (see above). A depleted mantle model age is an estimate of the time at which magmas are separated from the mantle source. Thus, this similarity indicates that the depleted upper mantle and young oceanic crusts are possible sources of these two igneous suites (see below). The model ages of other individual samples of TTG and Sanukitoid suites are similar, falling between 2.6 and 2.8 Ga, suggesting different levels of contamination of the lower continental crust.
2. The model ages of High-K granites fall between 2.7 and 2.9 Ga, which is different from their emplacement and crystallization age.

Geodynamic implications

Francistown plutonic rocks intruded between 2.7 and 2.65 Ga and, according to major/trace element geochemical study (Kampunzu et al. 2003) and Sm–Nd isotopic data, this process involved partial melting of depleted upper mantle (Sanukitoid suite), subducting oceanic plate (TTG suite), and continental crust (High-K granites). In a short time interval (about 50 Ma) products of partial melting of both ocean crust and continental crust occurred in the same place, which cannot be explained by a continental rift model. The isotope data further support the model of an active continental margin, involving the subduction of an oceanic plate (Limpopo oceanic plate) underneath a continental plate (Tokwe continental plate). This model is in good agreement with major and trace element geochemical data (Kampunzu et al. 2003). The Sanukitoid suite is enriched in mobile incompatible elements and thus has high Cs/La, Ba/La ratios, suggesting the addition of mobile elements in the mantle wedge by aqueous fluids. This is a characteristic of magmas along subduction zones (e.g. Gill 1981). A cross-section of the sketch presenting the relationships between the geneses of the Francistown plutonic rocks in a plate convergent environment is shown in Fig. 8.

Conclusions

The following conclusions can be drawn from the above discussion:

1. The Sr isotopic system within the Francistown plutonic rocks has been disturbed by post crystallization thermo-tectonic events. Such events include migmatization as well as reactions between circulating solutions and granitic rocks.
2. Three igneous suites (TTG, Sanukitoid suites and High-K granites) were identified in the Francistown arc complex. The former two suites were formed at ~2.7 Ga and the High-K granites at ~2.65 Ga.

3. The TTG suite was generated by partial melting of a young subducting oceanic plate. However, the parental magma of the TTG suite underwent crystal fractionation coupled with crustal contamination (up to 14%) en route to the surface and/or in crustal magma chambers. The LA-TTG sub-suite was the product of the fractionation and contamination of HA-TTG sub-suite.
4. The Sanukitoid suite was formed by partial melting of the mantle wedge of the overriding continental plate. It may be contaminated by continental crust to the level of 10%.
5. High-K granite magma originated from partial melting of TTG suite, probably the Francistown LA-TTG sub-suite, and/or lower continental crust of the overriding continental plate.
6. The plutonic rocks in the Francistown area were formed in a continental plate convergent environment, where a young oceanic plate subducted underneath an old continental plate (Fig. 8).

Acknowledgements Funding for this study was provided by the University of Botswana (Faculty of Science Research and Publication Committee Grant No: R101). The sampling was done during a previous project under the support of the Kaapvaal Craton Research Funds (Project R442). The authors thank Dr. S. Duchene and Dr. Peucat for their very helpful reviews.

References

Allègre CJ, Rousseau D (1984) The growth of the continents through geological time studied by the Nd isotopic analysis of shales. Earth Planet Sci Lett 67:19–34

Arth JG, Hanson GN (1972) Quartz diorites derived by partial melting of eclogite or amphibolite at mantle depths. Contrib Mineral Petrol 37:161–174

Arth JG, Hanson GN (1975) Geochemistry and origin of the early Precambrian crust of northeastern Minnesota. Geochim Cosmochim Acta 39:325–362

Bagai Z, Armstrong R, Kampunzu AB (2002) U–Pb single zircon geochronology of granitoids in the Vumba granite–greenstone terrain (NE Botswana): implication for the Archaean Zimbabwe craton. Precamb Res 118:149–168

Barker F (1979) Trondhjemite: definition, environment and hypotheses of origin. In: Bark F (ed) Trondhjemites, Dacites, and related rocks. Elsevier, Amsterdam, pp 1–12

Barker F, Millard HT, Knight RJ (1979) Reconnaissance geochemistry of devonian Island—arc volcanic and intrusive rocks, west Shasta district, California. In: Bark F (ed) Trondhjemites, Dacites, and related rocks. Elsevier, Amsterdam, pp 531–545

Bickle MJ, Orpen JL, Nisbet EG, Martin A (1993) Structure and metamorphism of the Belingwe greenstone belt and adjacent granite–gneiss terrain: the tectonic evolution of an Archaean craton. In: Bickle MJ, Nisbet EG (eds) The geology of the Bilingwe greenstone belt: a study of the evolution of Archaean continental crust. Geological Society of Zimbabwe Special publication No. 2, pp 39–68

Brook C, Hart SR, Wendt T (1972) Realistic use of two-error regression treatments as applied to rubidium–strontium data. Revi Geophys Space Phys 10:551–577

Cahen L, Snelling NJ, Delhal J, Vail JR (1984) The geochronology and evolution of Africa. Clarendon, Oxford, p 512

Carney JN, Aldiss DT, Lock NP (1994) The geology of Botswana. Geological Survey Department, Botswana

Chatupa JC (1999) Gold prospects and occurrences in the greenstone belts of Botswana. Mineral Resources Report no. 14. Geological Survey Department, Botswana

Condie KC (1975) Mantle-plume model for the origin of Archaean greenstone belts based on trace element distributions. Nature 258:413–414

Coward MP, James PR, Wright L (1976) Northern margin of the Limpopo orogenic belt, southern Africa. Geol Soc Am Bull 87:601–611

DePaolo DJ (1981a) Neodymium isotopes in the Colorado Front range and crust–mantle evolution in the Proterozoic. Nature 291:193–196

DePaolo DJ (1981b) Trace element and isotopic effects of combined wallrock assimilation and fractional crystallisation. Earth Planet Sci Lett 53:189–202

DePaolo DJ, Wasserburg GJ (1976) Nd isotopic variations and petrogenetic models. Geophys Res Lett 3:249–252

Dickin A (1995) Radiogenic isotope geology. Cambridge University Press, London

Dirks PHGM, Jelsma HA (2002) Crust–mantle decoupling and the growth of the Archaean Zimbabwe craton. J Afr Earth Sci 34:157–166

Dodson MH, Compston W, Williams IS, Wilson JF (1988) A search for ancient detrital zircon in Zimbabwean sediments. J Geol Soc Lond 145:977–983

Dodson MH, Williams IS, Kramers JD (2001) The Mushandike granite: further evidence for 3.4 Ga magmatism in the Zimbabwe craton. Geol Mag 138:31–38

Drummond MS, Defant MJ (1990) A model for trondhjemite–tonalite–dacite genesis and crustal growth via slab melting: Archaean to modern comparisons. J Geophys Res 95:21503–21521

Editorial (2003) Standards for publication of isotope ratio and chemical data in chemical geology. Chem Geol 202:1–4

Evans AM (1993) Ore geology and industrial minerals. An introduction, 3rd edn. Blackwell, London

Faure G (1986) Principles of isotope geology. Wiley, New York, pp 117–246

Frei R, Blenkinsop TG, Schönberg R (1999) Geochronology of the late Archaean Razi and Chilimanzi suites of granites in Zimbabwe: implications for the late Archaean tectonics of the Limpopo Belt and Zimbabwe craton. South Afr J Geol 2:55–63

Gill JB (1981) Orogenic andesites and plate tectonics. Springer, Berlin Heidelberg New York

Govindaraju K (1994) Compilation of working values and sample description for 383 geostandards. Geostandard Newslett (special issue) 18:1–158

Hanson GN, Goldich SS (1972) Early Precambrian rocks in the Saganaga Lake-Northern Light Lake area, Minnesota-Ontario; Pt. 2, Petrogenesis. In: Doe BR, Smith DK (eds) Studies in Mineralogy and Precambrian geology. Geological Society of America Memorandum 135:179–192

Horstwood MSA, Nesbitt RW, Noble SR, Wilson JF (1999) U–Pb zircon evidence for an extensive early Archean craton in Zimbabwe: a reassessment of the timing of craton formation, stabilization, and growth. Geology 27:707–710

Hughes CJ (1982) Igneous petrology. Elsevier, Amsterdam

Ito E, White WM, Göpel C (1987) The O, Sr, Nd isotope geochemistry of MORB. Chem Geol 62:157–176

Jelsma HA, Dirks PHGM (2000) Tectonic evolution of a greenstone sequence in northern Zimbabwe: sequential early stacking and pluton diapirism. Tectonics 19:135–152

Jelsma HA, Dirks PHGM (2002) Neoarchaean tectonic evolution of the Zimbabwe craton. In: Fowler CMR, Ebinger CJ, Hawkesworth CJ (eds) The early earth: physical, chemical and biological development. Special Publications Geological Society London 199:183–211

Jelsma HA, Vinyu ML, Valbracht PJ, Davies GR, Wijbrans JR, Verdurmen EAT (1996) Constraints on Archaean crustal evolution of the Zimbabwe craton: a U–Pb zircon, Sm–Nd and Pb–Pb whole-rock isotope study. Contrib Mineral Petrol 124:55–70

Kagami H, Yokose H, Honma H (1989) $^{87}Sr/^{86}Sr$ and $^{143}Nd/^{144}Nd$ ratios of GSJ rock reference samples, JB-1a, JA-1 and JG-1a. Geochem J 23:209–214

Kamber BS, Ewart A, Collerson KD, Bruce MC, McDonald GD (2002) Fluid-mobile trace element constraints on the role of slab melting and implications for Archaean crustal growth models. Contrib Mineral Petrol 144:38–56

Kampunzu AB, Tombale AR, Zhai M, Bagai Z, Majaule T, Modisi MP (2003) Major and trace element geochemistry of plutonic rocks from Francistown, NE Botswana: evidence for a Neoarchaean continental active margin in the Zimbabwe craton. Lithos 71:431–460

Key RM (1976) The geology of the area around Francistown and Phikwe, Northeast and Central Districts, Botswana. Geological Survey of Botswana District Memoir 3, 121p

Kusky TM (1998) Tectonic setting and terrane accretion of the Archaean Zimbabwe craton. Geology 26:163–166

Litherland M. (1975) The geology of the area around Maitengwe, Sebina and Tshesebe, Northeast and Central Districts, Botswana. Geological Survey of Botswana District Memoir 2, 133p

Liu Y, Gao S, Yuan H, Zhou L, Liu X, Wang X, Hu Z, Wang L (2004) U–Pb zircon ages and Nd, Sr, and Pb isotopes of lower crustal xenoliths from North China Craton: insights on evolution of lower continental crust. Chem Geol 211:87–109

Ludwig KR (2001) Users manual for isoplot/ex, a geochronological toolkit for Microsoft Excel, rev. 2.49. Special Publication No. 1a, Berkeley Geochronology Center pp 1–45

Majaule T, Davis DW (1998) U–Pb zircon dating and geochemistry of granitoids in the Mosetse area, NE Botswana, and tectonic implications. In: 50th anniversary international conference abstract volume, Geological Survey of Botswana, pp 46–48

Martin H (1993) The mechanisms of petrogenesis of the Archaean continental crust—comparison with modern processes. Lithos 30:373–388

McCourt S, Vearncombe JR (1992) Shear zones of the Limpopo Belt and adjacent granitoid–greenstone terranes: implications for late Archaean collision tectonics in southern Africa. Precamb Res 55:553–570

McCourt S, Kampunzu AB, Armstrong RA, Bagai Z (2004) The crustal architecture of Archaean terranes in Northeastern Botswana. South Afr J Geol 107:147–158

McCulloch MT, Bennett VC (1993) Evolution of the early earth: constraints from ^{143}Nd–^{142}Nd isotopic systematics. Lithos 30:237–255

Michard A, Gurriet P, Soudant M, Albarède F (1985) Nd isotopes in Franch phanerozoic shales: external vs internal aspects of crustal evolution. Geochim Cosmochim Acta 49:601–610

Mkweli S, Kamber B, Berger M (1995) Westward continuation of the Craton-Limpopo Belt tectonic break in Zimbabwe and new age constraints on the timing of the thrusting. J Geol Soc Lond 152:77–83

Nägler TF, Kramers JD (1998) Nd isotopic evolution of the upper mantle during the Precambrian: models, data and the uncertainty of both. Precamb Res 91:233–252

Nägler TF, Kramers JD, Kamber BS, Frei R, Prendergast MDA (1997) Growth of subcontinental lithospheric mantle beneath Zimbabwe started at or before 3.8 Ga; Re–Os study on chromites. Geology 25:983–986

Petford N, Atherton M (1996) Na-rich partial melts from newly underplated basaltic crust: the Cordillera Blanca Batholith, Peru. J Petrol 37:1491–1521

Ranganai RT, Kampunzu AB, Atekwana EA, Paya BK, King JG, Koosimile DI, Stettler EH (2002) Gravity evidence for a larger Limpopo Belt in southern Africa and geodynamic implications. Geophys J Int 149:F9–F14

Rapp RP (1997) Heterogeneous source for Archaean granitoids: experimental and geochemical evidence. In: de Wit MJ, Ashwal LD (eds) Greenstone belts. Clarendon, New York, pp 267–279

Rapp RP, Watson EB, Miller CF (1991) Partial melting of amphibolite/eclogite and the origin of Archean trondhjemites and tonalites. Precamb Res 94:4619–4633

Roberts RG, Sheaham PA (1988) Ore deposit models. Geological Association of Canada

Rollinson H (1993) Using geochemical data: evaluation, presentation, interpretation. Longman Scientific & Technical, New York, pp 215–264

Rushmer T (1991) Partial melting of two amphibolites: contrasting experimental results under fluid-absent conditions. Contrib Mineral Petrol 107:41–59

Shirey SB, Hanson GN (1984) Mantle-derived Archean monzodiorites and trachyandesites. Nature 310:222–224

Shirey SB, Hanson GN (1986) Mantle heterogeneity and crustal recycling in Archean granite–greenstone belts: evidence from Nd isotopes and trace elements in the Rainy Lake area, Superior Province, Ontario, Canada. Geochim Cosmochim Acta 50:2631–2651

Stern RA, Hason GN, Shirey SB (1989) Petrogenesis of mantle-derived LILE-enriched Archean monzodiorite and trachyandesites (sanukitoids) in southwestern Superior Province. Canad J Earth Sci 26:1688–1712

Stern RA, Hanson GN (1991) Archean High-Mg granodiorite: a derivative of light rare earth element-enriched monzodiorite of mantle origin. J Petrol 32:201–238

Tatsumi Y (1981) Melting experiments on a high-magnesian andesite. Earth Planet Sci Lett 54:357–365

Taylor PN, Kramers JD, Moorbath S, Wilson JF, Orpen JL, Martin A (1991) Pb/Pb, Sm–Nd and Rb–Sr geochronology in the Archean Craton of Zimbabwe. Chem Geol (Isot Geosci Sect) 87:175–196

Thirwall MF (1991) Long-term reproducibility of multicollector Sr and Nd isotope ratio analysis. Chem Geol 94:85–104

Tombale AR (1992) The geology, geochemistry and metallogeny of the Tati Greenstone belt, northeastern Botswana. Ph.D.Thesis, Memorial University of Newfoundland, Canada, pp 1–383

Van Breemen O, Dodson MH (1972) Metamorphic chronology of the Limpopo Belt, southern Africa. Bull Geol Soc Am 83:2005–2018

Wasserburg G, Jacobsen SB, De Paolo DJ, McCulloch MT, Wen T (1981) Precise determination of Sm/Nd ratios, Sm and Nd isotopic abundances in standard solutions. Geochim Cosmochim Acta 45:2311–2323

Whalen JB, Percival JA, McNicoll VJ, Longstaffe FJ (2002) A mainly crustal origin for tonalitic granitoid rocks, Superior province, Canada: implications for Late Archean tectonomagmatic processes. J Petrol 43:1551–1570

Wilson JF, Bickle MJ, Hawkesworth CJ, Martin A, Nisbet EG, Orpen JL (1978) Granite–greenstone terrains of the Rhodesian Archean Craton. Nature 271:23–27

Wilson JF (1990) A craton and its cracks: some of the behaviour of the Zimbabwe block from the Late Archean to the Mesozoic in response to horizontal movements, and the significance of some of its mafic dyke fracture patterns. J Afr Earth Sci 10:483–501

Wilson JF, Nesbitt RW, Fanning CM (1995) Zircon geochronology of Archaean felsic sequences in the Zimbabwe craton: a revision of greenstone stratigraphy and a model for crustal growth. In: Coward MP, Ries AC (eds) Early Precambrian Processes, Geological Society of London Special Publication 95:109–126

Wyllie PJ, Wolf MB, van der Laan SR (1997) Conditions for formation of tonalites and trondhjemites: magmatic sources and products. In: de wit MJ, Ashwal LD (eds) Greenstone belts. Clarendon, New York, pp 256–266